CrossMark

LncRNA-135528 inhibits tumor progression by up-regulating CXCL10 through the JAK/STAT pathway

Peng Wang[2] · Xiaobin Peng[2] · Jingjing Zhang[2] · Zhen Wang[1] · Jiaxue Meng[1] · Bohong Cen[1] · Aimin Ji[1] · Shuai He[1,3]

Abstract

Spontaneous tumor regression can be observed in many tumors, however, studies related to the altered expression of lncRNA in spontaneous glioma regression are limited, and the potential contributions of lncRNAs to spontaneous glioma regression remain unknown. To investigate the biological roles of lncRNA-135528 in spontaneous glioma regression. The cDNA fragment of lncRNA-135528 was obtained by rapid-amplification of cDNA ends (RACE) technology and cloned into the plvx-mcmv-zsgreen-puro vector. Additionally, we stably silenced or overexpressed lncRNA-135528 in G422 cells by transfecting with siRNA against lncRNA-135528 or lncRNA-135528 overexpression plasmid. Then, we examined lncRNA-135528 overexpressing and lncRNA-135528 silencing on glioma cells and its effects on CXCL10 and JAK/STAT pathways. The main findings indicated that lncRNA-135528 promoted glioma cell apoptosis, inhibited cell proliferation and arrested cell cycle progression; the up-regulation of lncRNA135528 led to significantly increased CXCL10 levels and the differential expression of mRNA associated with JAK/STAT pathway in glioma cells. lncRNA-135528 can inhibit tumor progression by up-regulating CXCL10 through the JAK/STAT pathway.

Keywords Spontaneous tumor regression · Glioma · LncRNA-135528 · CXCL10 · JAK/STAT pathways

Background

Glioma is one of the most common types of adult brain tumors, with high morbidity and mortality [1–4]. Although multi-dimensional treatments, including surgical resection, radiotherapy and chemotherapy, have been developed, the infiltrating growth pattern of glioma leads to poor prognostic outcomes. The median survival time in patients with glioblastoma multiform (GBM), which is the most malignant tumor type of glioma, is less than 15 months [5]. Thus, a better understanding of molecular pathogenesis and mechanisms of glioma generation is urgently needed to develop more effective treatments.

The spontaneous regression of malignancies is a phenomenon in which a proven tumor partially or completely disappears without any substantial treatment [6]. Since Everson and Cole first reported the spontaneous tumor regression in 1967 [7], more than 1000 case reports of spontaneous tumor regression have been published, these articles reported on common associated tumors, including glioma [8–10], choriocarcinoma [11], neuroblastoma [12], renal cell carcinoma [13], melanoma [14], sarcoma [15], bladder carcinoma [16] and osteogenic sarcoma [17]. Recent studies have reported that almost all tumors can undergo spontaneous regression [18–25]. Spontaneous tumor regression may be triggered by immune regulation, induced differentiation, hormone mediation, elimination of carcinogens, psychological factors, apoptosis and epigenetic mechanisms [6].However, the underlying mechanism causeing a potentially lethal tumor

✉ Shuai He
hs43555@163.com

1 Zhujiang Hospital, Southern Medical University, Guangzhou 510282, China

2 The Fifth Affiliated Hospital of Southern Medical University, Guangzhou 510900, China

3 Guangdong Provincial Key Laboratory of New Drug Screening, School of Pharmaceutical Sciences, Southern Medical University, Guangzhou 510515, China

strikingly shift course without any intervention remains unknown.

Due to low incidence of spontaneous tumor regression and the difficulty of establishing a model, most reports are case studies and phenomenon analyses, and studies on the molecular mechanism of establishing tumor regression models of spontaneous tumor regression are rare. Current available methods for CTVT and surgical transplantation are limited by specific tumor models, high technical threshold and difficulties in the surgical transplant [26, 27]. Therefore, the establishment of a simple, reproducible spontaneous tumor regression model with a high success rate is necessary to study the mechanism of spontaneous tumor regression.

Long non-coding RNA (lncRNA) is a non-encoded RNA with a length greater than 200 nucleotides. Based on different lncRNA profiles during mammalian development and in various diseases [28, 29], researchers have demonstrated that lncRNAs perform important tasks throughout the course of life. However, lncRNAs responsive to spontaneous tumor regression have rarely been reported. Therefore, it is necessary to investigate the biological roles of lncRNAs in spontaneous tumor regression.

Materials and methods

Cell culture

U87MG cells (human malignant glioblastoma multiforme cell line) were purchased from ATCC (Manassas, Virginia, USA), G422 cells (mouse malignant glioblastoma multiforme cell line) were obtained from Land biotechnology (Guangzhou, China). The cells were grown and cultured with DMEM supplemented with 10% FBS (Invitrogen, USA) in 5% CO_2 incubator at 37 °C.

Tumor regression models

BALB/c mice (male, 4–6 weeks old, approximately 20 g) were obtained from the Experimental Animal Center at Southern Medical University (Guangzhou, China) and maintained in a sterile environment in accordance with standard animal care guidelines. The experiments were performed according to national regulations. The mice were administered cyclosporine soft capsule [30–32] (HuaDong Medicine Co., Ltd, China) (40 mg/kg/day), and the U87 (6×106) cells were subcutaneously inoculated on the right back of mice three days later. After 8 days of inoculation, the mice were randomly divided into two groups (A and B) when the tumor was successfully established. Group A continued to receive treatment with cyclosporine soft capsules (40 mg/kg/day), while group B ceased to receive treatment. Digital calipers (Mitutoyo, Japan) was used to measure tumor length (L) and short diameter (W)

every three days (tumor volume $V = LW^2/2$), and the IVIS Spectrum Imaging System (Bruker, USA) was used to monitor the growth process of fluorescent labeled U87 tumor. The mice were sacrificed, and the tumor tissue was collected when group B showed tumor regression of approximately 50%.

RNA extraction

Total RNA was extracted from U87 tumor sample according to the manufacturer's instructions of Trizol®LS (Invitrogen, Stockholm, Sweden) and the quantity and quality was confirmed by a NanoDrop 1000 Spectrophotometer. The total amount of RNA obtained was not significantly different between the samples.

LncRNA microarray assay

Isolation of total RNA from tumor sample was performed as described above. Sample labeling and array hybridization were performed according to the Arraystar microarray-based gene expression analysis protocol (Agilent Technology). The Arraystar Mouse LncRNA Microarray V3.0 which is designed for the global profiling of mouse lncRNA and protein-coding transcripts can detected approximately 35,923 lncRNAs and 24,881 coding transcripts. Agilent Scanner G2505B was uded to scan the arrays, and Agilent Feature Extraction software (version 11.0.1.1) was used to analyze the acquired array images, and GeneSpring GX v12.1 software (Agilent Technologies) was used to quantile normalization and subsequent data processing. The microarray assay was carried out by Kangchen Bio-tech (Shanghai, China) and The procedures were conducted as previously described [33].

Quantitative reverse transcription-polymerase chain reaction (RT-qPCR)

To initiate cDNA synthesis, the PrimeScript™ RT Reagent Kit with gDNA Eraser (Perfect Real Time) (TaKaRa, Japan) was used to reverse transcribe (RT) 2 µl of total RNA according to the manufacturer's instructions. The real-time monitoring of the DNA amplification reaction was performed using a Real-Time PCR Detection System (Light Cycler 480, Roche) and SYBR®Premix Ex Taq™ (Tli RnaseH Plus) (TaKaRa, Japan). β-actin was performed as the internal control and used to normalize the results. The primers used for RT-qPCR are listed in Table 1.

Gene ontology (GO) and kyoto encyclopedia of genes and genomes (KEGG) pathway analysis

GO categories and GeneSpring GX software (http://www.geneontology.org) were used to determine processes or

Table 1 The primers used in RT-qPCR analysis

Genes	Primers	Tm (℃)	PCR length (bp)
β-actin (M)	F:5′ GTACCACCATGTACCCAGGC3′ R :5′AACGCAGCTCAGTAACAGTCC3	60	247
ENSMUST00000124148	F:5′AAGCCTGCTGCTACTGATGG3′ R:5′GGAAATGCCTGTATTCTGGATG3	60	65
uc009bpw.2	F:5′GAAATGTGACTCCACCCAAGG3′ R:5′TGGACCTCCTTGCCATTCA3	60	148
AK1544040	F:5′TGTTCGTCCCACCTCCTATCA3′ R:5′GTAAGTGCCTGGAAACTCCCTAT3	60	181
ENSMUST00000125649	F:5′CGATGACAAGCTGAGGGACA3′ R:5′GCCTTCTTGCTGATCATATTTCTG3	60	118
ENSMUST00000131925	F:5′CCTCGGAAAGAGGGAGAGATC3′ R:5′CAGGCATTGAAACAAAACGGA3	60	50
NR_038007	F:5′ ACATACCGCATCCCGAAAC3′ R:5′ TTCCGTGTCAATCGAGGCT3	60	120
ENSMUST00000132304	F:5′GGCGCTCCCAGAACAAAC3′ R:5′CGTTCGCAGACAGCTTAGACA3	60	140
Scg2	F:5′GCCCCATAGAGGAGAAAATAGAG3′ R:5′ ACTGCCCACAGCATTCACTAAC3	60	218
Hs6st2	F:5′ ACCAATGACTACATAGGGAGCG3′ R:5′ AGCATAACACTGAATCAAAAGGC3	60	210
Mybpc2	F:5′ TGATGGAGGACAGCCAGTGAC3′ R:5′ GAAGACCCGCATCTCATAAAGG3	60	151
Cldn3	F:5′ ACCGTACCGTCACCACTACCAG3′ R:5′ GTTTCTTTGTCCATTCGGCTTG3	60	212
Myoz1	F:5′ CATTGACCTACTGGCATACGG3′ R:5′ GCTCAACCAGGGAATAGGG3	60	223
lncRNA-135528	F:5′ AAGACACAGAGATAGGAGGG3′ R:5′ GGTCACAGCAACAGAAAGAA3	60	131
CXCL10	F:5′ CCCTCTCGCAAGGACGGTC3′ R:5′ AATGATCTCAACACGTGGGC3	60	124
JAK1	F:5′ TGTTCTCTATGAGGTCATGGT3′ R:5′ TCCAGTTTTTTCCGCTTCAGT3	60	111
JAK2	F:5′ AGTCTTGGCCAAGGTACTT3′ R:5′ TTCGAAGAAAGACTCTGAATA3	60	141
STAT2	F:5′ CAGATACACAGTTTTCAGTC3′ R:5′ ACCAGTCCTTTGGAGATGT3	60	138
STAT3	F:5′ GAGTTCAAGCACCTGACCCT3′ R:5′ AGGCCTTGGTGGTACACCTCA3	60	131
18srRNA	F:5′ CCTGGATACCGCAGCTAGGA3′ R:5′ GCGGCGCAATACGAATGCCCC3	60	112

functional categories which were differentially expressed [34]. The GO annotation system uses a controlled and hierarchical vocabulary to assign function to genes or gene products in any organism [35]. The lower the P-values, the more significant the GO terms ($P \leq 0.05$ was considered statistically significant).

We performed pathway analysis to map genes to KEGG for the differentially expressed mRNAs (http://www.genome.jp/kegg/). The *P*-value (EASE-score, Fisher P-value or Hypergeometric *P*-value) denotes the significance of the pathway correlated to the conditions (the recommended *P*-value cut-off is 0.05).

RACE and vector construction

LncRNA-135528 is located on chromosome fifth, starting at txstart:92331840-txend:92346770, with a total length of 1815 bases. To clone the full-length cDNA of lncRNA-135528, we performed the 5′-RACE and 3′-RACE analyses using a SMARTer™ RACE cDNA Amplification

Kit (Takara, Japan) according to the manufacturer's instructions. Then, the lncRNA-135528 cDNA was used as the template for PCR amplification and the recovery of PCR products by DNA gel recovery kit (Dongsheng Biotech, China). Then the recovery products and pLVX-mCMV-ZsGreen-puro vector were digested with Bamhi/noti. T4 DNA Ligase (Takara, Japan) was used to link the target fragment with pLVX-mCMV-ZsGreen-puro vector of the enzyme-cutting recovery and to form the vector pLVX-mCMV-ZsGreen-puro-lncRNA-135528 and Sequencing verification.

SiRNA screening

G422 cells were seeded into 6-well plates (CORNING, China) at a density of 5×10^4 cells/well, and maintained at 37 °C in a humidified incubator containing 5% CO_2. When the rate of cell confluence reaches 40%, the cells were transfected with siRNA for 6 h. After that, the old medium was replaced with the new medium. 24 h later, the cells was collected and siRNAs efficiency was detected by quantitative PCR. Three small interfering RNAs were designed and synesized to target various region of lncRNA-135528 gene expression by Sigama, USA and NC_AS was designed as control group (Table 2). β-actin was performed as the internal control and used to normalize the results. PCR primers are shown in Table 1.

Transfection

To obtain lncRNA135528 silence and overexpression of G422 cells. siRNA, siRNA-NC, pLVX-mCMV-ZsGreen-puro, or pLVX-mCMV-ZsGreen-puro-lnc-RNA135528 was transfected into G422 cells. The siRNAs and vectors were tra-nsfected into G422 cells by using Lipofectamine 2000 (Invitrogen, USA) in accordance with the manufacturer's instructions.

TUNEL assay

Apoptosis analysis in tumor tissue was detected by TUNEL method. Mice were killed after 14 days of inoculation and tumor tissue samples were removed and fixed in 4% paraformaldehyde. After paraffin embedding, slicing and dewaxing, the TUNEL reaction was performed according to the manufacturer's instructions of In situ Apoptosis Detection Kit (Abcam, UK). The color of TUNEL-positive cells were brown.

Immunostaining

Proliferation analysis in tumor tissue was tested by Ki67 immunostaining. Mice were sacrificed after 14 days of inoculation and tumor tissue samples were removed and fixed in 4% paraformaldehyde. Paraffin sections were incubated with anti-Ki-67 (1:50) overnight at 4 °C, which was followed by secondary antibodies [IFKine Red AffiniPure Donkey Anti-Rabbit IgG (H + L)] at 20–37 °C for 1 h. Photos were taken by fluorescence microscope (DMI6000B, leica, Germany).

CCK-8 assay

Cell proliferation in vitro was performed using CCK-8 assays. The five experimental groups (cell, NC, lncRNA, siRNA-NC and siRNA) of G422 cells were seeded into 96-well plates (CORNING, China) at a density of 1×10^4 cells/well, with 3 replicate wells per group. The cells were cultured in a humidified 5% CO_2 incubator at 37 °C for 3 days in succession. Then 10 μl CCK-8 solution was added to each well. After 4 h, the spectrophotometric absorbance was measured at 450 nm for each sample and the mean value was calculated. Cell Counting Kit-8 was purchased from Invitrogen, USA.

Table 2 siRNAs

[line]Name	Sequence: (5′-3′)	Size	Epsilon 1/ (mMcm)	MW g/mol	OD
Si 1	GAGAUGAAUUACCCUGUGGDTDT	21	203.1	6694	
Si 1_AS	CUCUACUUAAUGGGACACCDTDT	21	205.4	6618	
Duplex of above				13,312	2.0
Si 2	UCACUAGAUCAUGAGCAGGDTDT	21	209.7	6599	
Si 2_AS	AGUGAUCUAGUACUCGUCCDTDT	21	211.5	6637	
Duplex of above				13,236	2.0
Si 3	CGAACUCAAGCAUCUUCUCDTDT	21	200.8	6625	
Si 3_AS	GCUUGAGUUCGUAGAAGAGDTDT	21	207.2	6611	
Duplex of above				13,266	2.0
NC	UUCUCCGAACGUGUCACGUdTdT	21	196.2	6563	
NC_AS	ACGUGACACGUUCGGAGAAdTdT	21	213.6	6712	
Duplex of above				13,275	2.0

Cell apoptosis assay

Cell apoptosis in vitro was assessed using a cell apoptosis kit, Annexin V-FITC Apoptosis Detection Kit (keygen, China). The experimental groups were harvested and washed twice in PBS, and re-suspended in Annexin V-FITC for 15 min in the dark. Then binding after 1× binding buffer and Propidium Iodide were added. Cell apoptosis was analyzed by BD caliber (BD, USA).

Cell cycle analysis

Cell cycle progression were analyses by Flow-cytometric. G422 cells were collected 48 h after transfection and washed twice in PBS and fixed in 70% ice-cold ethanol at 4 °C overnight. After washing with PBS, add 500 μl PBS containing 50 μg/ml bromide (PI), 100 μg/ml RNase A, 0.2% Triton X-100, 4 °C to incubate for 30 min, data were collected using a BD Calibur flow cytometer.

Western blot analysis

Western blotting was performed as per standard protocols. Tissue or cells were lysed with RIPA buffer (Beyotime, China),. and protein concentration were measured by BCA Protein Assay Kit (KeyGEN BioTECH, China). Soluble proteins were loaded into 8% SDS-PAGE and electrophoresis. Then the proteins were transferred onto PVDF membrane (Millipore,USA) and blocked for 2 h with Blocking Buffer (Beyotime, China) in room temperature. Primary antibodies were incubated Overnight, 4 °C and secondary antibodies for 1 h, room temperature. For visualization of bands, we used the BeyoECL Plus Western Blotting Detection Reagents (Beyotime, China). GAPDH(aksomics, CHINA) as loading control. The following antibodies were used in this study: Anti-CXCL10 Antibody (Sigma, USA), Goat Anti-Rabbit IgG (H + L) Antibody (Sigma, USA), Anti-Ki67

antibody (abcam, UK), IFKine Red AffiniPure Donkey Anti-Rabbit IgG (H + L) (Abbkine, CHANA), Anti-JAK1 antibody (abcam, UK), Anti-JAK2 antibody (abcam, UK), Anti-STAT2 antibody (abcam, UK), Anti- STAT3 antibody (abcam, UK), Goat Anti-Rabbit IgG (H + L) (Mouse/Human ads-HRP) (Abbkine, CHANA). Expression ratios were calculated with Image J.

Statistical analysis

Data were presented as mean ± SEM, and Statistical significance was determined by one-way analysis of variance (ANOVA) followed by LSD or Dunnett's T_3 test in SPSS software (version 19.0, SPSS, Chicago, IL, USA). All samples were run in triplicate and experiments were repeated at least three times unless specified. A P values of < 0.05 was considered statistically significant.

Results

Tumor regression model

The Fig. 1 shows that the tumor was obviously uplifted on the skin, with a volume of approximately 250 mm³ after 8 days. As shown in Fig. 2, after stopping the administration of cyclosporine, the tumor in group A continued to increase, and the tumor in group B began to subside, on day 8, there was no statistically significant difference between the two groups (P > 0.7), but on days 11 and 14, there was a statistically significant difference between the two groups (P < 0.05, P < 0.05). Additionally, the fluorescence intensity of group A increased with increasing tumor size, and the fluorescence intensity of group B decreased with tumor decline (Fig. 3). Repeated experiments generated similar results. These results show that the tumor regression models were successful.

Fig. 1 Morphology and size of tumor tissues in vivo and in vitro
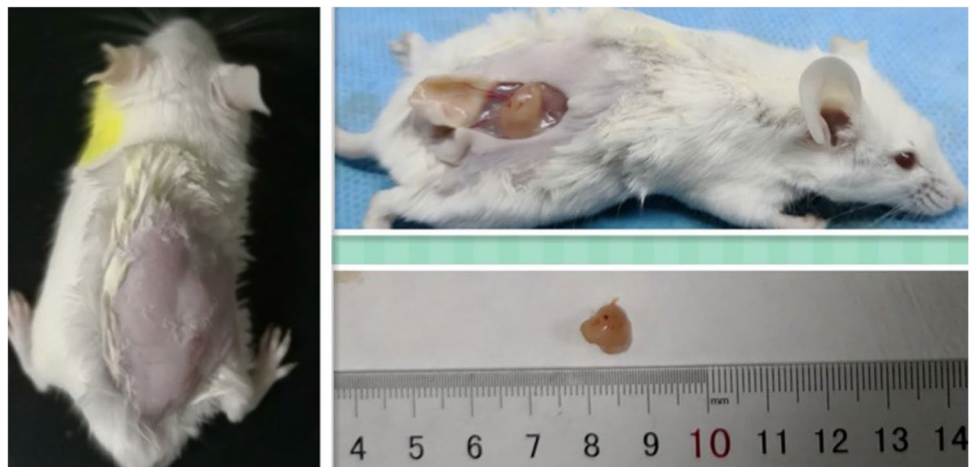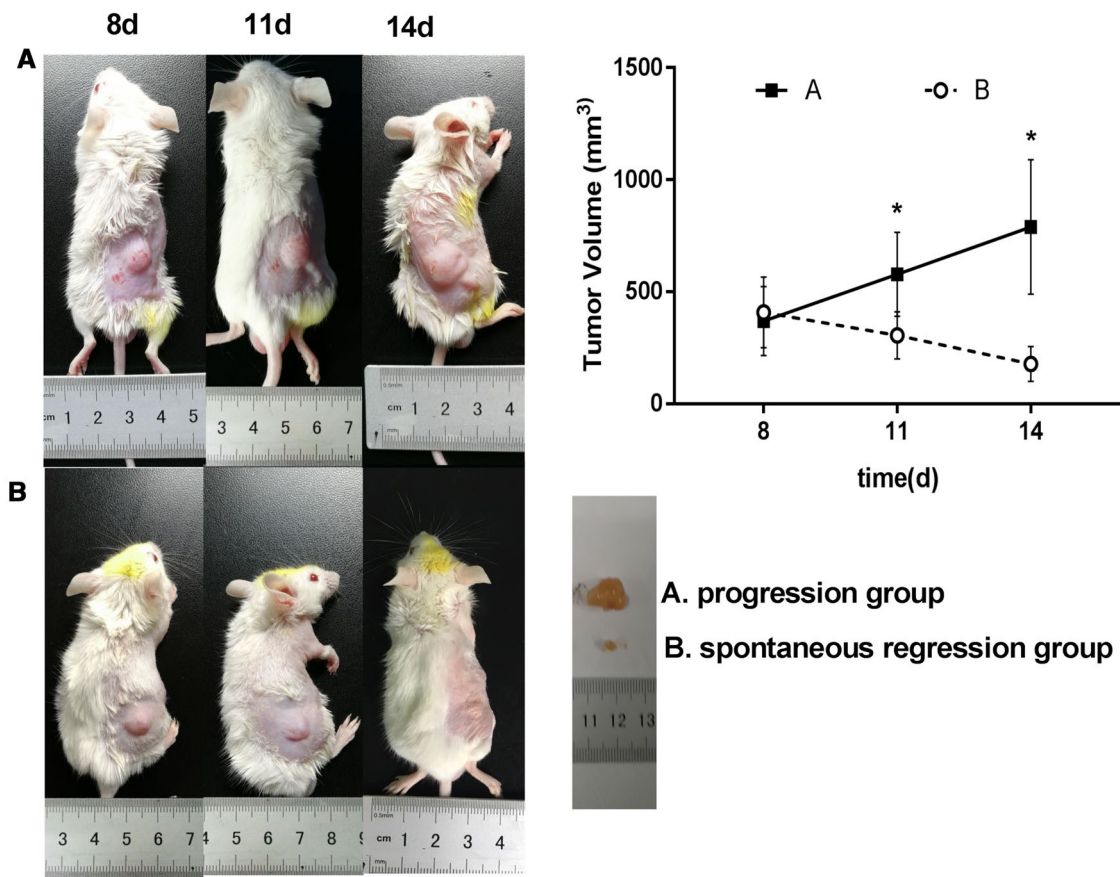
Fig. 2 Changes of tumor volume in the spontaneous glioma regression model. **a** represents the progression group, **b** represents the spontaneous regression group. The number of animals for each experiment were 5

Proliferation and apoptotic analysis in tumor tissue

The expression of ki67 in the regression group was significantly decreased compared with the progression group (Fig. 4a). TUNEL assay shows that cell apoptosis significantly increased in the regression group compared with the progression group (Fig. 4b). These results further validated the tumor regression models were set up successfully.

Differentially expressed lncRNAs and mRNAs in spontaneous regressive and progressive tumors

Figure 5 showed the differently expressed lncRNA and mRNA associated with spontaneous glioma regression. The lncRNA expression profiles revealed that approximately 15,791 lncRNAs (7605 up- and 8186 down-regulated) were differentially expressed ($\geq$ twofold-change, P $\leq$ 0.05), and 67 lncRNAs (66 up- and 1 down-regulated) displayed greater than 50-fold changes (Table 3). The mRNA expression profiles revealed approximately 11,173 mRNAs (4929 up- and 6244 down-regulated) that were significantly differentially expressed ($\geq$ twofold-change, P $\leq$ 0.05), and 97 mRNAs

(95 up- and 2 down-regulated) and displayed greater than 50-fold changes (Table 4).

Real-time quantitative PCR validation

To independently validate the chip results, quantitative real-time polymerase chain reaction (RT-qPCR) was performed to analyze the expression of 7 lncRNAs and 5 mRNAs (the detailed microarray analysis results was shown in Additional file 1: Table S1) randomly selected from the differentially expressed lncRNAs and mRNAs. As shown in Fig. 6, lnRNA uc009bpw.2, AK154404, ENSMUST00000124148, ENSMUST00000125649 and mRNA Cldn3, Mybpc2, Myoz1 were up-regulated, lnRNA ENSMUST00000131925, ENSMUST00000132304, NR_038007 and mRNA Scg2, Hs6st2 were down-regulated, these results were consistent with the microarray analysis.

GO analysis and pathway analysis

The genes corresponding to the down-regulated mRNAs included 5325 genes involved in biological processes, 5387
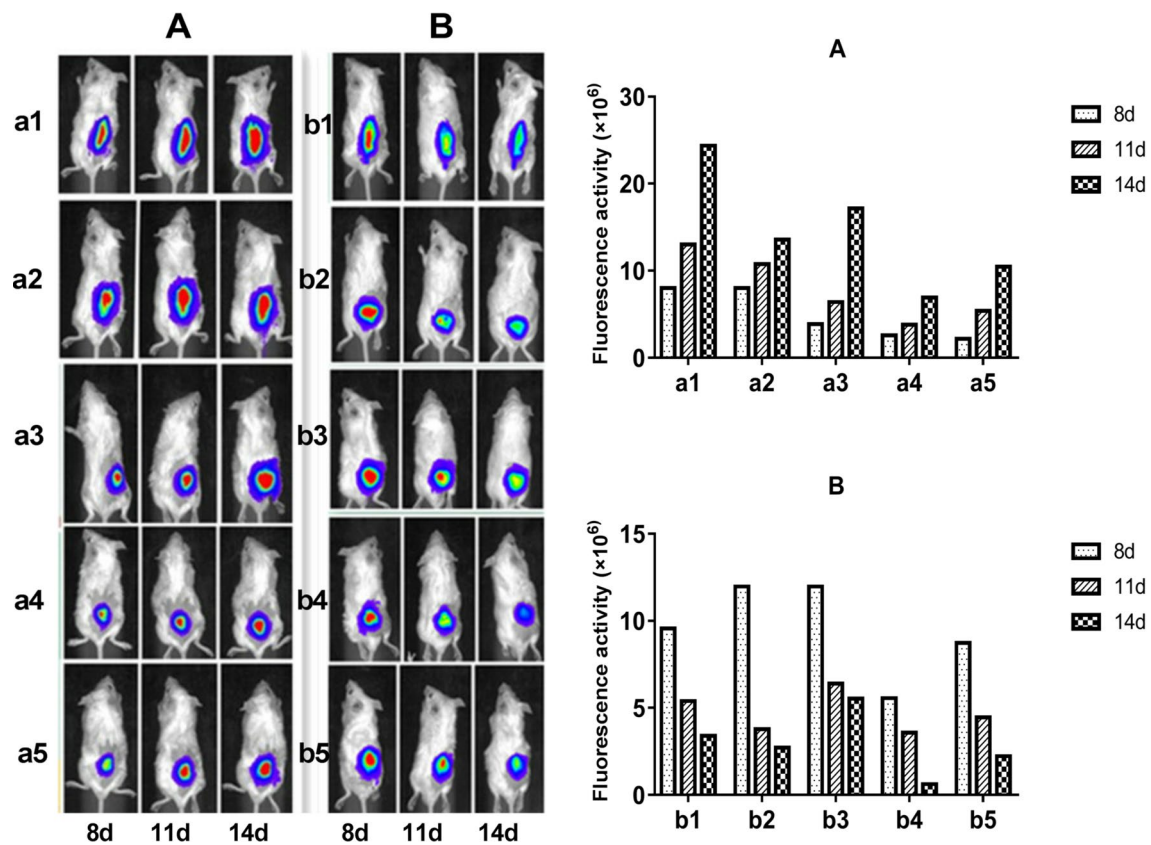
Fig. 3 Changes of fluorescence value of mice subcutaneous tumor in the spontaneous glioma regression model. **a** represents the progression group, **b** represents the spontaneous regression group. a1, a2, a3, a4, a5 represent different mice in Group A, b1, b2, b3, b4 and b5 represent different mice in Group B

genes involved in cellular components and 5,280 genes involved in molecular functions. In contrast, the genes corresponding to the up-regulated mRNAs included 4398 genes involved in biological processes, 4460 genes involved in cellular components and 4360 genes involved in molecular functions. As shown in Fig. 7a, "T cell chemotaxis" (GO: biological processes), "nuclear telomere cap complex" (GO: cellular components), and "telomerase activity" (GO: molecular functions) were the highly enriched GOs targeted by up-regulated transcripts, while "inactivation of MAPK activity" (GO: biological processed), "PRC1 complex" (GO: cellular components) and "JUN kinase binding" (GO: molecular function) were the highly enriched GOs targeted by down-regulated transcripts (Fig. 7b). Among these terms, T cell chemotaxis was highly relative to immunity, while inactivation of MAPK activity was highly associated with glioma apoptosis [36–38], suggesting tumor suppression in spontaneous glioma regression. Simultaneously, we identified 5923 genes (3036 up- and 2887 down-regulated) associated with cell proliferation and cell apoptosis (Additional file 2: Table S2). Among these genes, 284 genes were involved in the regulation of neuron apoptotic process, 21

genes regulated cell proliferation in the brain, 8 genes were associated with regulation of glial cell proliferation, and 582 genes were closely associated with the apoptotic or proliferative processes of immune cells.

We performed a pathway analysis of the differentially expressed mRNAs by using the KEGG database. The pathway analysis revealed 61 pathways corresponding to the up-regulated transcripts ($P \leq 0.05$), and 7 pathways were related to immune responses and inflammatory reactions. In contrast, 78 pathways corresponded to the down-regulated transcripts ($P \leq 0.05$), and 12 pathways were associated with cancer pathways (Additional file 3: Table S3).

The expression of lncRNA-135528 and CXCL10 in tumors of spontaneous regression model

To verify the differential expression of lncRNA-135528 and CXCL-10 in tumor regression models, the expressions of lncRNA-135528 and CXCL-10 in the different groups was analyzed by qRT-PCR and Western blotting. As shown in Fig. 8a, the expression levels of lncRNA-135528 in the tumor regressive group was significantly decreased

Fig. 4 Proliferation and apoptotic analysis in tumor tissue. **a** immunofluorescence staining analysis of Ki67 in tumor tissues. **b** Representative images for TUNEL assay to determine apoptosis cell in tumor tissues. Yellow arrow, proliferating cells; red arrow, apoptotic cells. (Color figure online)
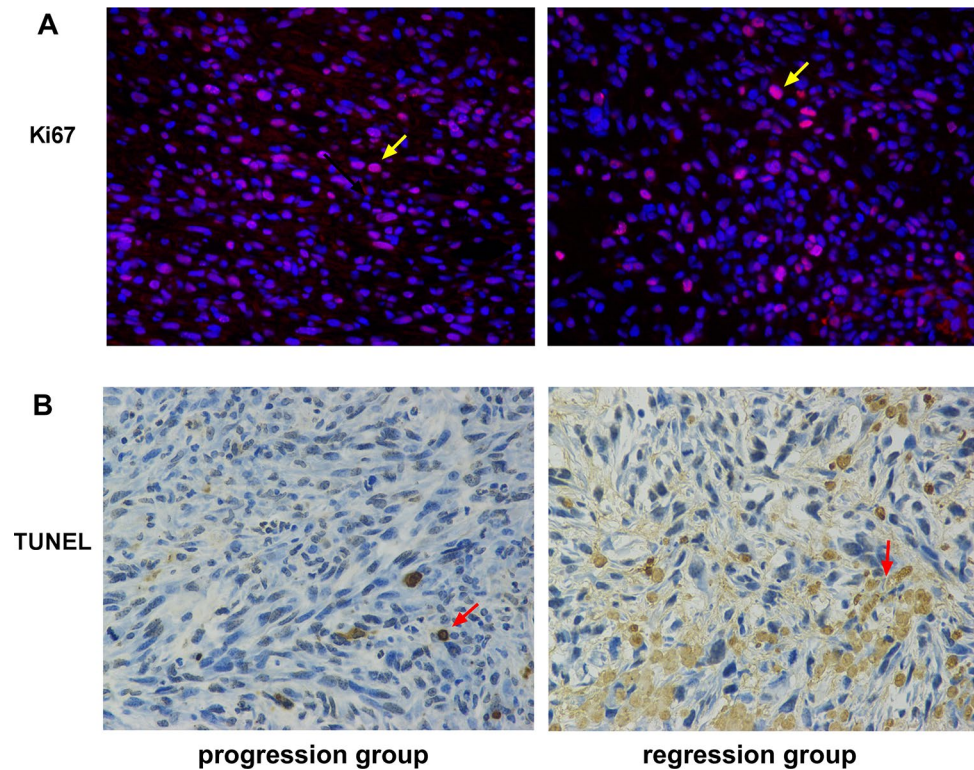
comparing with the tumor progression group (P < 0.05). As shown in Fig. 8b–d the expression of CXCL-10 mRNA and protein in the tumor regression group was significantly decreased comparing with the tumor progression group (P < 0.05, P < 0.05). The results showed that lncRNA-135528 and CXCL-10 expression were up-regulated in the tumor regression group, while stable in the tumor progression group. This was consistent with the results of microarray analysis.

LncRNA-135528 full-length clone and Vector construction

The cDNA fragment of lncRNA-135528 was obtained by RACE technology. The full-length lncRNA-135528 cDNA was cloned into the plvx-mcmv-zsgreen-puro vector, and BLAST analysis showed that lncRNA-135528 was successfully cloned into the plvx-mcmv-zsgreen-puro vector, and blast 100% was consistent with known sequences on NCBI (Additional file 4: Fig. S1). Thus, this construct can be used in subsequent experiments.

SiRNA3 (25 nM) had the highest inhibition rate

We designed 3 small interfering RNAs targeting different regions of lncRNA-135528 sequencing. The glioma cell line G422 was infected with different concentrations of siRNAs. At 24 h after infection, all three lncRNA-135528

siRNAs reduced lncRNA-135528 expression comparing with the negative control group. The inhibition rate of siRNA1-25 nM, siRNA1-50 nM, siRNA3-100 nM, siRNA2-25 nM, siRNA2-50 nM, siRNA2-100 nM, siRNA3-25 nM, siRNA3-50 nM, siRNA3-100 nM was 25%, 5%, 32%, 3%, 43%, 42%, 75%, 26% and 26% respectively, but siRNA3-25 nM had the highest efficiency, with an inhibition rate of 75% (Fig. 9). Thus, we used siRNA3-25 nM for further biological experiments.

LncRNA-135528 inhibited cell proliferation, promoted cell apoptosis and arrested cell cycle progression

To investigate the biological roles of lncRNA-135528 in glioma, we stably silenced or overexpressed lncRNA-135528 in G422 cells by transfecting siRNA against lncRNA-135528 or the lncRNA-135528 overexpression plasmid. As shown in Fig. 11a, the expression of lncRNA-135528 in the lncRNA group (lncRNA-135528 overexpression group) was significantly increased (P < 0.05) compared with the cell group, while the expression of lncRNA-135528 in the siRNA group (lncRNA-135528 knockdown group) was significantly decreased (P < 0.05), indicating successful transfection.

In order to study the effect of lncRNA-135528 on cell proliferation, we conducted the cck-8 assay. As shown in Fig. 10a, b, the proliferation of G422 cells in the lncRNA group was drastically inhibited (P < 0.05) compared with
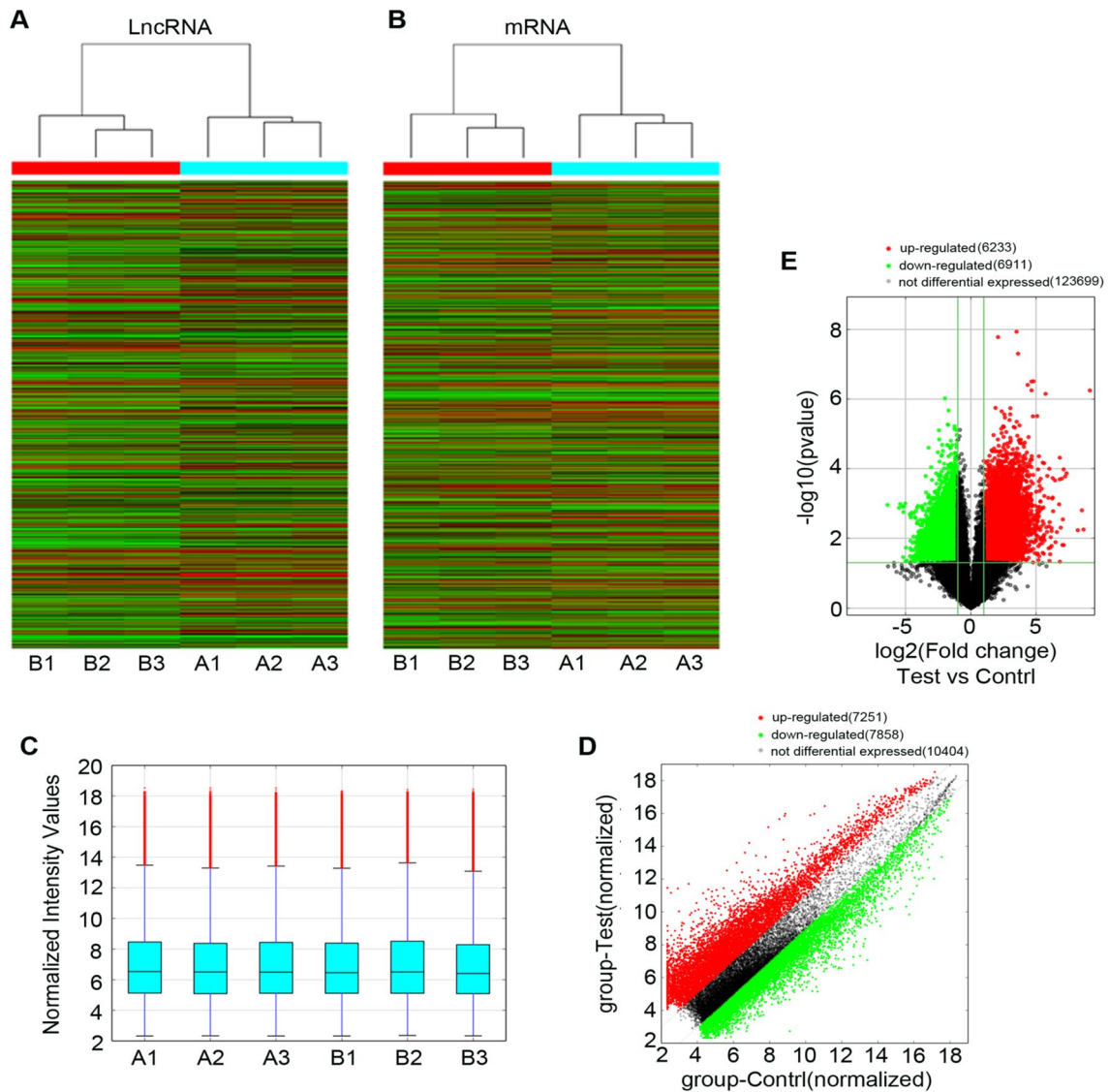
Fig. 5 RNA expression profiles in spontaneous regressive U87 tumors and progressive tumors. **a, b** Hierarchical clustering of lncRNAs (**a**) and mRNAs (**b**). The red and the green shades indicate the expression above and below the relative expression, respectively, across all the samples. **c** Box plots of lncRNAs to visualize the distri-bution of a dataset. **d** Scatter plot of the lncRNAs to assess the vari-ation between chips. **e** Volcano plot of the lncRNAs. "Red" indicates up-regulated expression, "green" indicates down-regulated expres-sion, and "black" represents transcripts with undifferentiated expres-sion. (Color figure online)

Table 3 The differentially expressed lncRNAs (long non-coding RNAs) in the spontaneous regressive U87 tumors implanted in BALB/c mice compared to progressive controls

Differentially expressed lncRNAs	Fold-change (≥ 2)	Fold-change (≥ 10)	Fold-change (≥ 50)	Fold-change (≥ 100)
Up-regulated	7605	1050	66	39
Down-regulated	8186	241	1	–

Table 4 The differentially expressed mRNAs (messenger RNAs) in the spontaneous regressive U87 tumors implanted in BALB/c mice compared to progressive controls

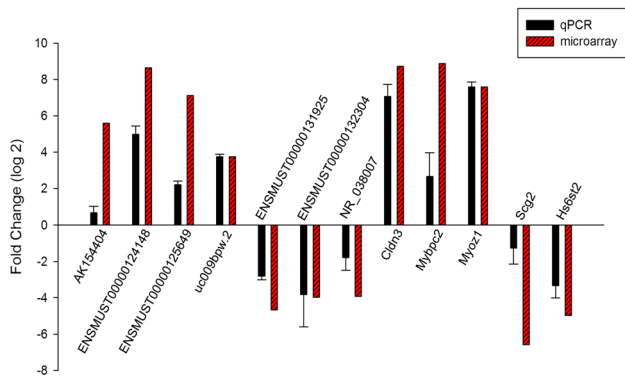| Differentially expressed mRNAs	Fold-change (≥ 2)	Fold-change (≥ 10)	Fold-change (≥ 50)	Fold-change (≥ 100)
Up-regulated	4929	746	95	37
Down-regulated	6244	233	2	–

Fig. 6 Validation of lncRNA microarray data by RT-qPCR. A total of seven differentially expressed lncRNAs and five differentially expressed mRNAs were randomly selected from the microarray to validate the accuracy of the microarray results by using RT-qPCR

the cell group, while the proliferation of G422 cells in the siRNA group was significantly enhanced (P < 0.05), suggesting that the ectopic expression of lncRNA-135528 inhibited G422 cell proliferation.

Apoptosis was detected by flow cytometry. As shown in Fig. 10c, e, comparing with the cell group, the apoptosis of G422 cells in lncRNA group was significantly enhanced (P < 0.05), while siRNA group decreased significantly (P < 0.05), suggesting that lncRNA-135528 overexpression promoted apoptosis of G422 cells.

In order to investigate the effect of lncRNA-135528 on cell cycle, we performed cell cycle analyses by flow cytometry. As shown in Fig. 10d, f, comparing with the cell group, the percentage of G1 cells decreased and the percentage of S-phase cells increased in the siRNA group, while the lncRNA group showed the opposite results. No significant changes in the percentage of cells were observed in the G1 or S phase in the NC, siRNA-NC and Blank groups (P > 0.05). These results suggest that lncRNA-135528 can arrested cell cycle progression.

Taken together, these findings suggest that lncRNA-135528 plays a role in the proliferation, apoptosis and cell cycle progression of G422 cells.

LncRNA-135528 regulates the JAK/STAT pathway by up-regulating CXCL10

As shown in Fig. 11e, f, the expression of CXCL10 mRNA and protein in the lncRNA group was significantly increased comparing with the cell group (P < 0.05, P < 0.05), while the expression of CXCL10 mRNA and protein in the siRNA group was decreased significantly (P < 0.05, P < 0.05). As shown in Fig. 11b–d, compared with the cell group, the expression of JAK1, JAK2, STAT2, STAT3 mRNA and protein was significantly increased in the lncRNA group

(P < 0.05, P < 0.05, P < 0.05, P < 0.05), while in the siRNA group was reversed. The schematic diagram was performed as described before [39] and shown in Fig. 12.

Discussion

Spontaneous tumor regression occurs in many types of human cancers. The mechanisms underlying spontaneous tumor regression may include immune mediation, tumor inhibition by growth factors and/or cytokines, hormonal mediation, induction of differentiation, tumor necrosis and/or angiogenesis inhibition, apoptosis and epigenetic mechanisms [6]. The present study reported the expression profile of lncRNAs and mRNAs in spontaneous U87 tumor regression models and the inhibitory effect of lncRNA-135528 on glioma activity and its molecular mechanism. The data obtained in the present study suggested that immune activation and tumor inhibition were possible underlying mechanisms. This finding is consistent with the results of other studies. Hicks et al. showed that spontaneous regression mice resisted high doses of cancer cells, and that this resistance was mediated by the rapid infiltration of leukocytes, including natural killer cells, macrophages, and neutrophils [40]. Moreover, Halliday et al. indicated that the overexpression of CD4+ T lymphocytes was related to the spontaneous regression of human skin tumors [41]. Rogozinskj et al. reported that the spontaneous regression of human papillomavirus-induced plane warts reportedly relies on immunological responses [42].

Due to low incidence of spontaneous tumor regression and the difficulty of establishing a model, most reports are case studies and phenomenon analyses [43, 44], it's necessary to establish a simple, reproducible spontaneous tumor regression model. In this study, U87 cells were subcutaneously inoculated on the right back of BALB/c mice to establish a spontaneous tumor regression model, and cyclosporin soft capsules were used to suppress the immune system in mice. Then, cyclosporin treatment was stopped after successful inoculation, and over time, the tumor began to undergo spontaneous regression. This model was reproducible and easy to operate, showing a high success rate.

In recent years, researchers have gradually unveiled the hidden functions of lncRNAs in complex gene networks. LncRNAs are no longer transcriptional noise in the transcriptome, but rather take center stage in both normal cellular processes and disease pathogenesis [45]. Owning to the abnormal lncRNA profiles in various tumors, lncRNAs play important roles in cancer biology. For example, increasing genome-wide profiling studies have demonstrated that lncRNAs are dysregulated in gliomagenesis and could be used to predict clinical phenotypes and prognosis in gliomas [46–48]. Moreover, several lncRNAs have been
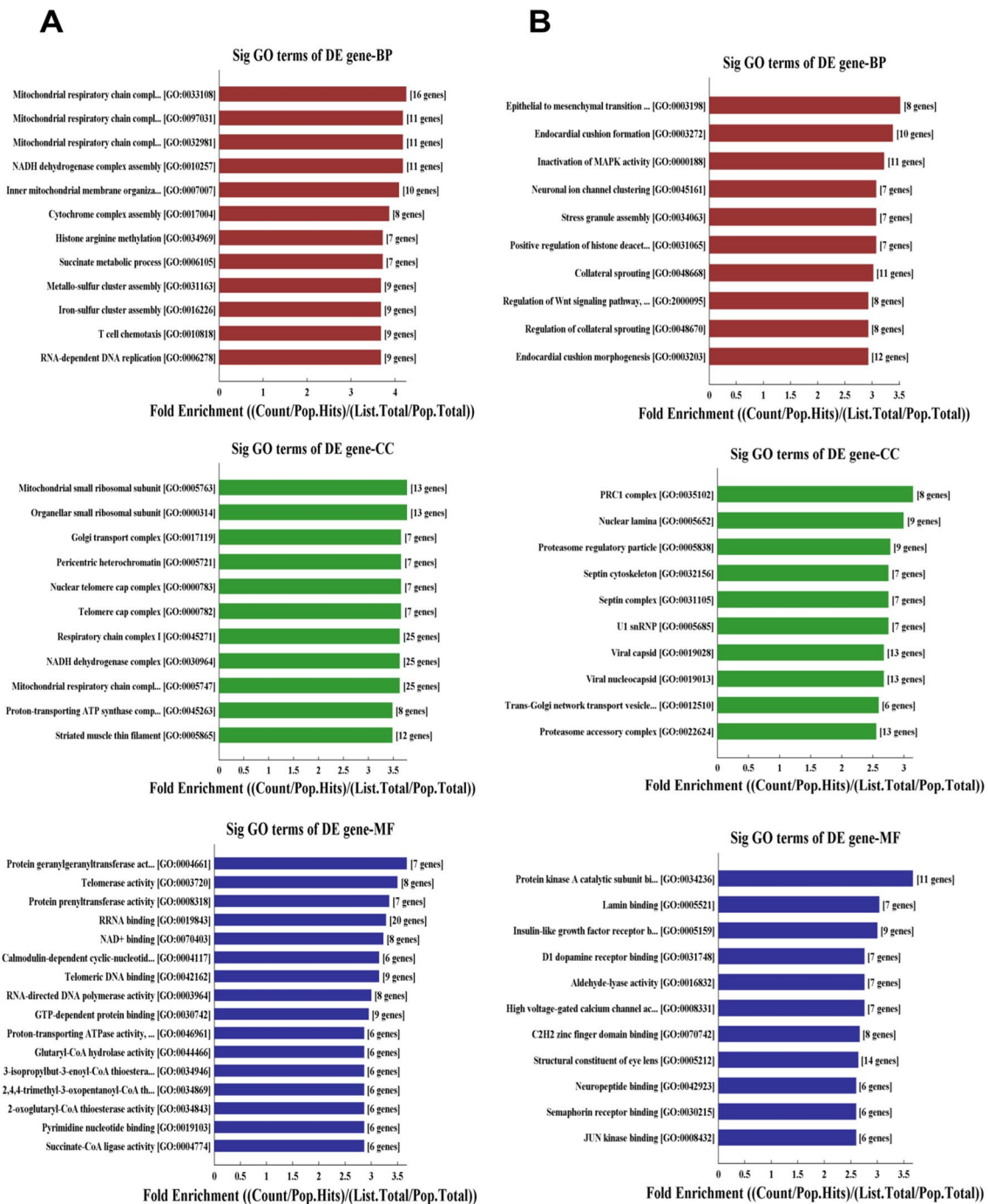
A

Sig GO terms of DE gene-BP

Sig GO terms of DE gene-CC

Sig GO terms of DE gene-MF

B

Sig GO terms of DE gene-BP

Sig GO terms of DE gene-CC

Sig GO terms of DE gene-MF

Fig. 7 The Gene ontology (GO) project provides a controlled vocabulary to describe gene and gene product attributes in any organism. **a** GO up-regulated. **b** GO down-regulated

demonstrated to possess functional significance in glioma, lncRNA HOTAIR acts as a prognostic factor for glioma patient survival [49]. Another well-known lncRNA H19 promoted invasion in glioma cells [50]. In this study, we found that silencing lncRNA-135528 inhibits the proliferation and promotes the apoptosis of glioma cells. However, this study used mouse microarray and mouse glioma cell line (G422)

to study the effects of the immune system on the regression of tumors during the course of tumor regression. Future studies could use human microarray and human glioma cell line (U87) to verify this finding and to further elucidate the molecular mechanism of tumor regression.

In the present study, we performed comprehensive lncRNA and mRNA expression profiling on the U87 tumors

Fig. 8 The expression of lncRNA-135528 and CXCL10 in tumors of spontaneous regression model. **a** The expression of lncRNA-135528 in tumor tissues of different groups. **b** The expression of CXCL10 mRNA in tumor tissues of different groups. **c, d** The expression of CXCL10 protein in tumor tissues of different groups. The data represent the means ± SEM. *p < 0.05 represent the significant differences between the progression group and the regression group
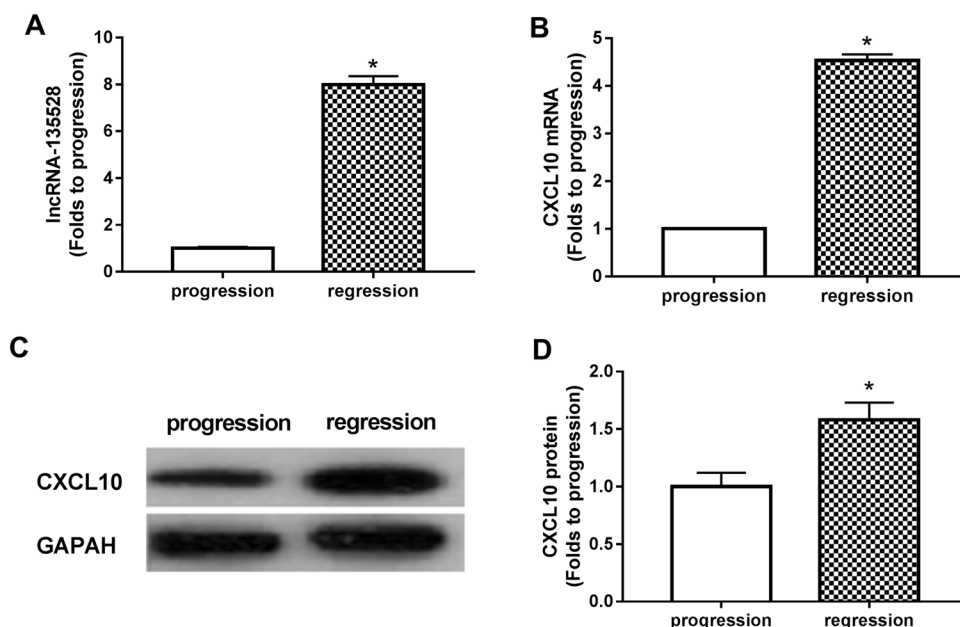
grown in BALB/c mice with spontaneous regression using microarray technology. The results showed that more than half of transcripts were involved in the regulation of cell proliferation or apoptosis, consistent with the direct cause of spontaneous tumor regression, suggesting that the rate of tumor cell proliferation was slower than that of tumor cell apoptosis. Moreover, among these proliferation-/or apoptosis-associated genes, approximately one-tenth of the transcripts were involved in the proliferation or apoptosis of immune cells. This suggests that there may be some factors triggering the immune system and then induce spontaneous

tumor regression. Identifying the key molecular elements will bring us one step closer to effectively curing or preventing cancer.

CXCL10 has important physiological and pathological effects and is involved in inflammatory, tumor, and immunological diseases [51]. Studies have shown that CXCL10 can play a role in tumor inhibition by promoting the aggregation and infiltration of lymphocytes in tumor tissue and activating lymphocyte function [52–56]. However, there are few studies on the role of CXCL10 in inhibiting glioma and its molecular mechanism. Chip information shows that CXCL10 was up-regulated 49 times in spontaneous tumor regression, and software predictions show that lncRNA-135528 has an interaction relationship with CXCL10. Thus, we selected lncRNA-135528 as the focus of the present study. This study showed that the overexpression of lncRNA-135528 can significantly up-regulate CXCL10 and that the JAK/STAT signal pathway was activated, while silencing lncRNA-135528 causes the opposite effect. Additionally, the overexpression of lncRNA-135528 inhibited cell proliferation, promoted cell apoptosis and arrested cell cycle progression, while silencing lncRNA-135528 inhibited the proliferation and promoted the apoptosis of glioma cells. This suggests that LncRNA-135528 inhibits tumor progression by up-regulating CXCL10 through JAK/STAT pathway.
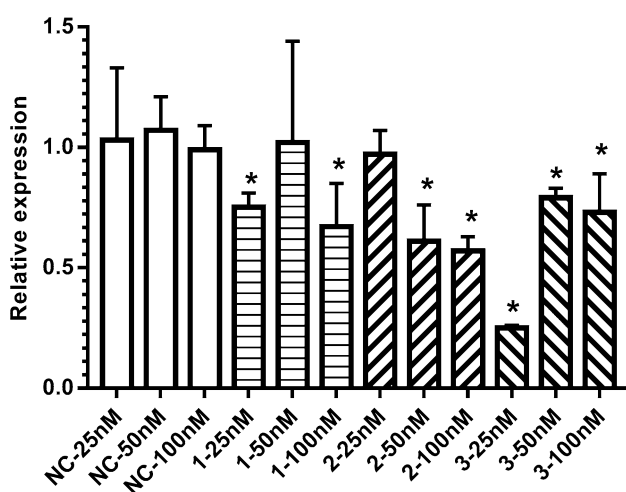
Fig. 9 SiRNA screening Notably, 1, 2, and 3 represent different siR-NAs, and 25, 50 and 100 nM represent different concentrations. The data represent the means ± SEM. *p < 0.05 represent the significant differences between the treated group and the cell group

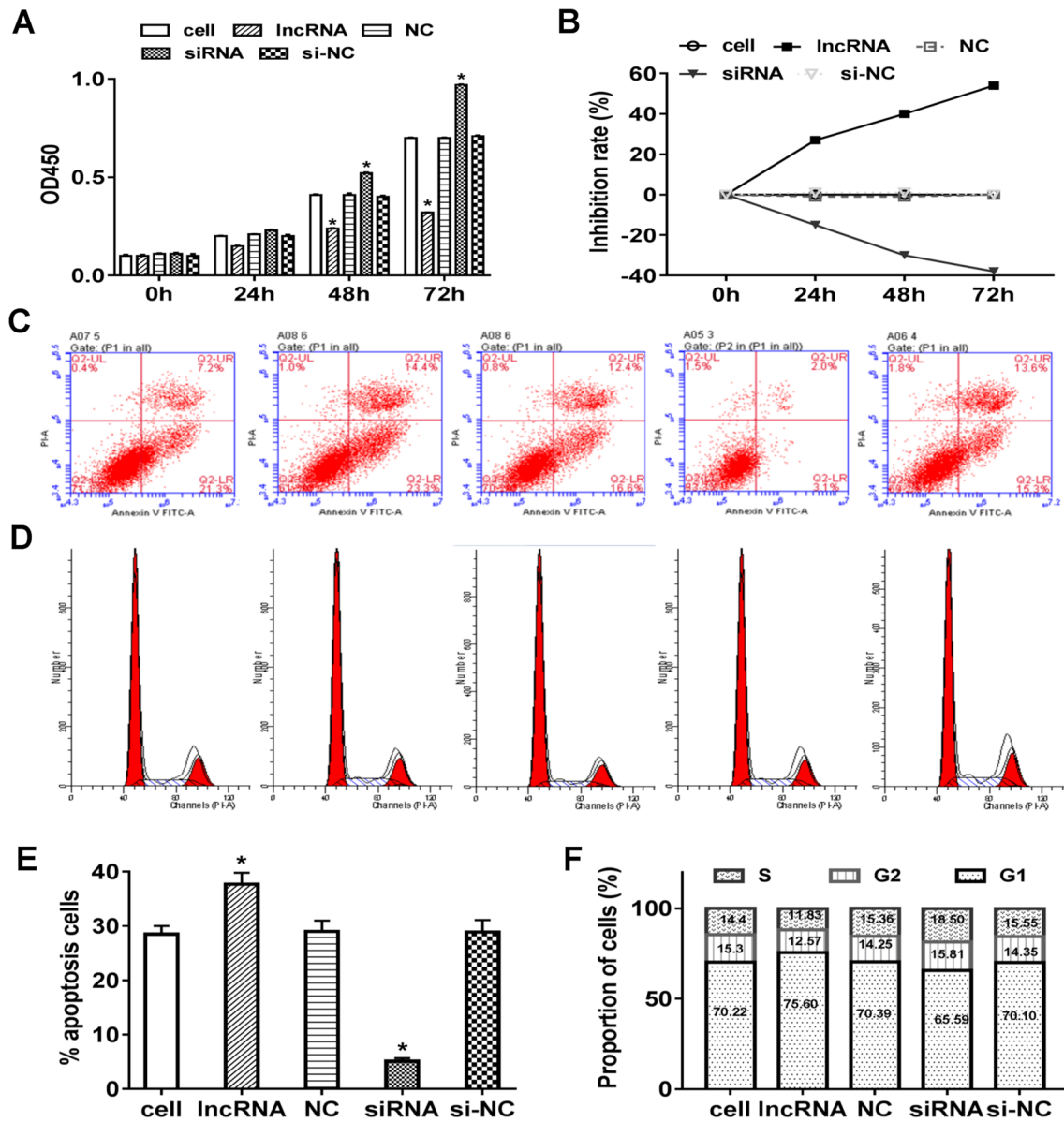Fig. 10 Effects of lncRNA-135528 on cell proliferation (**a, b**), cell apoptosis (**c, e**) and cell cycle (**d, f**). **a** MTS detection of lncRNA-135528 gene sensitivity in G422 cells. **b** Inhibitory rate of lncRNA-135528 gene sensitivity in G422 cells. **c, e** Apoptotic results for the cell group, lncRNA group, NC group, siRNA group and si-NC group. **d** Cell cycle results for the cell, lncRNA, NC, siRNA and si-NC groups. **f** Percentage of G1, G2 and S-phase cells in the cell cycle. The data represent the means ± SEM. *$p < 0.05$ represent the significant differences between treated groups and the cell group

Fig. 11 Effects of lncRNA on CXCL10 and JAK/STAT pathways. **a** The expression differences of lncRNA-135528 in the different groups. The differential expression of mRNA (**b**) and protein (**c, d**) associated with JAK/STAT pathway in the different groups. The expression of CXCL10 mRNA (**e**) and CXCL10 protein (**f**) in the different groups. Cell group represents the cells that have not been treated, lncRNA, NC, siRNA, si-NC represent cells transfected by pLVX-mCMV-ZsGreen-puro-lncRNA135528, pLVX-mCMV-ZsGreen-puro, siRNA or siRNA-NC respectively. The data represent the means ± SEM. *$p < 0.05$ represent the significant differences between treated groups and the cell group
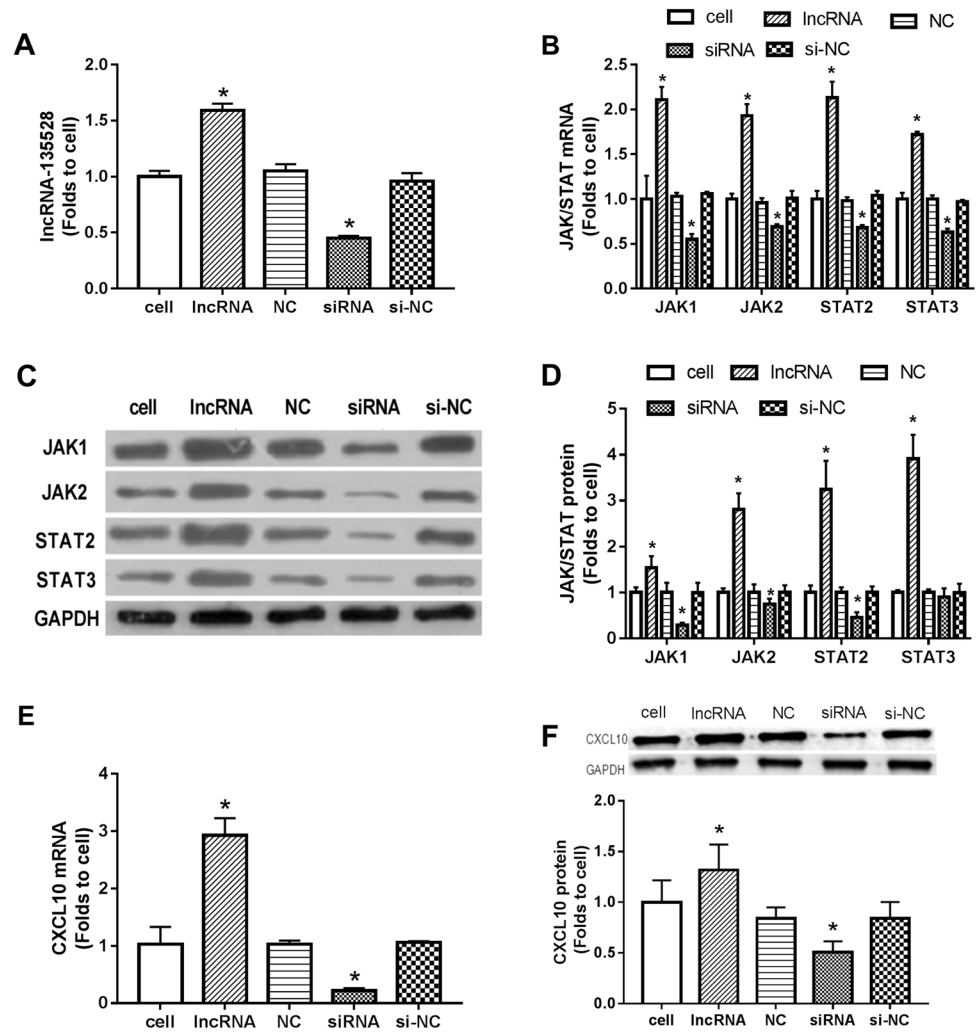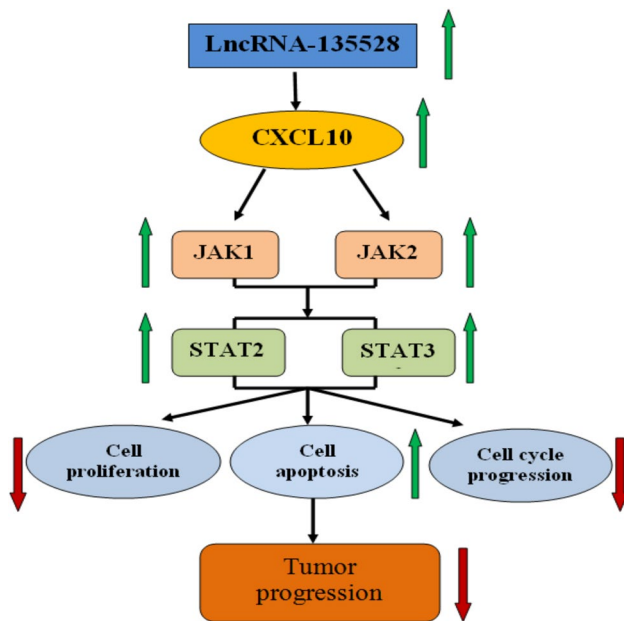
Fig. 12 Mechanism diagram of lncRNA-135528 inhibiting glioma progression. Overexpression of lncRNA-135528 can up-regulate CXCL10, followed by the JAK/STAT signal pathway activation, and then inhibited cell proliferation, promoted cell apoptosis and arrested cell cycle progression of tumor cells, and finally inhibited tumor progression

Conclusion

lncRNA-135528 can inhibit tumor progression by up-regulating CXCL10 through the JAK/STAT pathway.

Data Availability Data sharing not applicable to this article as no datasets were generated or analyzed during the current study.

Compliance with ethical standards

Conflict of interest The authors declare no competing financial interests.

Ethics approval The project was approved by the ethics committee of Southern Medical University (committee's reference number: SYXK 2016–0167).

References

1. Guo Z, Li G, Bian E, Ma CC, Wan J, Zhao B (2017) TGF-beta-mediated repression of MST1 by DNMT1 promotes glioma malignancy. Biomed Pharmacother 94:774–780
2. Kugler W, Buchholz F, Kohler F, Eibl H, Lakomek M, Erdlenbruch B (2005) Downregulation of Apaf-1 and caspase-3 by RNA interference in human glioma cells: consequences for erucylphosphocholine-induced apoptosis. Apotosis 10:1163–1174
3. Lobon-Iglesias MJ, Santa-Maria LV, Puerta RP et al (2018) Tumor dissemination through surgical tracts in diffuse intrinsic pontine glioma. J Neurosurg Pediatr. https://doi.org/10.3171/2018.6.PEDS17658
4. Miyauchi JT, Tsirka SE (2018) Advances in immunotherapeutic research for glioma therapy. J Neurol 265:741–756
5. Holland EC (2000) Glioblastoma multiforme: the terminator. Proc Natl Acad Sci USA 97:6242–6244
6. Papac RJ (1998) Spontaneous regression of cancer: possible mechanisms. In Vivo 12:571–578
7. Everson TC (1967) Spontaneous regression of cancer. Prog Clin Cancer 3:79–95
8. Ishihara M, Yamamoto K, Miwa H, Nishi M (2017) Spontaneous complete regression of a brain stem glioma pathologically diagnosed as a high-grade glioma. Child Nerv Syst 33:2177–2180
9. Pruzan NL, de Alba CA, Gorovoy IR, Hoyt C (2015) Spontaneous regression of a massive sporadic chiasmal optic pathway glioma. J Child Neurol 30:1196–1198
10. Rozen WM, Joseph S, Lo PA (2008) Spontaneous regression of low-grade gliomas in pediatric patients without neurofibromatosis. Pediatr Neurosurg 44:324–328
11. Schilder JN (1992) Spontaneous regression of cancer; a description of 7 cases. Ned Tijdschr Geneeskd 136:2521–2525
12. Brodeur GM (2018) Spontaneous regression of neuroblastoma. Cell Tissue Res. https://doi.org/10.1007/s00441-017-2761-2
13. Janiszewska AD, Poletajew S, Wasiutynski A (2013) Spontaneous regression of renal cell carcinoma. Contemp Oncol (Pozn) 17:123–127
14. Kappauf H, Esser G (2018) Metachronous spontaneous remission of melanoma lung metastasis and mediastinal lymph node metastases. Oncol Res Treat 41:135–138
15. Tsunezuka H, Miyata N, Furuya T, Konishi E, Inoue M (2018) Spontaneous regression of primary pulmonary synovial sarcoma. Ann Thorac Surg 105:e129–e131
16. Mancebo JM, de la Pena J, Hidalgo L et al (1985) Spontaneous regression of cutaneous metastases of transitional cell carcinoma of the bladder. Arch Esp Urol 38:497–501
17. Ghatalia P, Morgan CJ, Sonpavde G (2016) Meta-analysis of regression of advanced solid tumors in patients receiving placebo or no anti-cancer therapy in prospective trials. Crit Rev Oncol Hematol 98:122–136
18. Cornish N, Maybury B, Otton S (2018) A four-year spontaneous remission of angioimmunoblastic T-cell lymphoma. Br J Haematol 180:176
19. Chin KM, Chan CY, Lee SY (2018) Spontaneous regression of pancreatic cancer: a case report and literature review. Int J Surg Case Rep 42:55–59
20. Uloza V, Ulozaite N, Vaitkus S, Sarauskas V (2017) Spontaneous regression of laryngeal carcinoma in 10 year old boy: a case report and review of literature. Int J Pediatr Otorhinolaryngol 103:10–13
21. Nogimori C, Yamamoto H, Nonaka K, Sazuka M, Hamaya H, Yamada H (2017) Spontaneous regression of lung cancer in an elderly patient: a case report. Nihon Ronen Igakkai Zasshi 54:555–559

22. Sait SF, Danzer E, Ramirez D, LaQuaglia MP, Paul M (2017) Spontaneous regression in a patient with infantile fibrosarcoma. J Pediatr Hematol Oncol. https://doi.org/10.1097/MPH.0000000000001013

23. Marques C, Queiroga H, Marques M, Moura C (2017) Spontaneous regression of a pulmonary adenocarcinoma after core needle biopsy. Autops Case Rep 7:20–25

24. Hori S, Tachihara M, Tamura D et al (2017) Spontaneous regression of epithelioid angiosarcoma in a young woman. Intern Med 56:3333–3339

25. Miyoshi Y, Takayashiki N, Satoh H (2017) Spontaneous regression of FDG/PET positive lung adenocarcinoma in an elderly man. Adv Respir Med 85:246–249

26. Chiang HC, Liao AT, Jan TR et al (2013) Gene-expression profiling to identify genes related to spontaneous tumor regression in a canine cancer model. Vet Immunol Immunopathol 151:207–216

27. Buijs M, Geschwind JF, Syed LH et al (2012) Spontaneous tumor regression in a syngeneic rat model of liver cancer: implications for survival studies. J Vasc Interv Radiol 23:1685–1691

28. Batista PJ, Chang HY (2013) Long noncoding RNAs: cellular address codes in development and disease. Cell 152:1298–1307

29. Rinn JL, Chang HY (2012) Genome regulation by long noncoding RNAs. Annu Rev Biochem 81:145–166

30. Cunha AM, Nascimento FS, Amaral JC, Konig S, Takiya CM, Neto V, Rocha E, Souza JP (2011) A murine model of xenotransplantation of human glioblastoma with immunosuppression by orogastric cyclosporin. Arq Neuropsiquiatr 69:112–117

31. Jivrajani M, Shaikh MV, Shrivastava N, Nivsarkar M (2014) An improved and versatile immunosuppression protocol for the development of tumor xenograft in mice. Anticancer Res 34:7177–7183

32. Krushelnycky BW, Farr-Jones MA, Mielke B, McKean JD, Weir BK, Petruk KC (1991) Development of a large-animal human brain tumor xenograft model in immunosuppressed cats. Cancer Res 51:2430–2437

33. Guo W, Lei W, Yu D et al (2017) Involvement of lncRNA-1700040D17Rik in Th17 cell differentiation and the pathogenesis of EAE. Int Immunopharmacol 47:141–149

34. Beissbarth T, Speed TP (2004) GOstat: find statistically overrepresented gene ontologies within a group of genes. Bioinformatics 20:1464–1465

35. Ashburner M, Ball CA, Blake JA et al (2000) Gene ontology: tool for the unification of biology. Gene Ontol Consort Nat Genet 25:25–29

36. Wang R, Deng D, Shao N et al (2018) Evodiamine activates cellular apoptosis through suppressing PI3K/AKT and activating MAPK in glioma. Onco Targets Ther 11:1183–1192

37. Yang J, Zhang JN, Chen WL et al (2017) Effects of AQP5 gene silencing on proliferation, migration and apoptosis of human glioma cells through regulating EGFR/ERK/p38 MAPK signaling pathway. Oncotarget 8:38444–38455

38. Wang A, Meng M, Zhao X, Kong L (2017) Long non-coding RNA ENST00462717 suppresses the proliferation, survival, and migration by inhibiting MDM2/MAPK pathway in glioma. Biochem Biophys Res Commun 485:513–521

39. Muhammad N, Bhattacharya S, Steele R, Ray RB (2016) Anti-miR-203 suppresses ER-positive breast cancer growth and stemness by targeting SOCS3. Oncotarget 7:58595–58605

40. Hicks AM, Riedlinger G, Willingham MC et al (2006) Transferable anticancer innate immunity in spontaneous regression/complete resistance mice. Proc Natl Acad Sci USA 103:7753–7758

41. Halliday GM, Patel A, Hunt MJ, Tefany FJ, Barnetson RS (1995) Spontaneous regression of human melanoma/nonmelanoma skin cancer: association with infiltrating CD4+ T cells. World J Surg 19:352–358

42. Rogozinski TT, Jablonska S, Jarzabek-Chorzelska M (1988) Role of cell-mediated immunity in spontaneous regression of plane warts. Int J Dermatol 27:322–326

43. Ooi KH, Cheo T, Soon G, Leong CN (2018) Spontaneous regression of locally advanced nonsmall cell lung cancer: a case report. Medicine (Baltimore) 97:e11291

44. Parks AL, McWhirter RM, Evason K, Kelley RK (2015) Cases of spontaneous tumor regression in hepatobiliary cancers: implications for immunotherapy? J Gastrointest Cancer 46:161–165

45. Li Y, Zhang J, Pan J et al (2018) Insights into the roles of lncRNAs in skeletal and dental diseases. Cell Biosci 8:8

46. Xu C, Qi R, Ping Y et al (2017) Systemically identifying and prioritizing risk lncRNAs through integration of pan-cancer phenotype associations. Oncotarget 8:12041–12051

47. Zhang XQ, Kiang KM, Wang YC et al (2015) IDH1 mutation-associated long non-coding RNA expression profile changes in glioma. J Neurooncol 125:253–263

48. Zhang X, Sun S, Pu JK et al (2012) Long non-coding RNA expression profiles predict clinical phenotypes in glioma. Neurobiol Dis 48:1–8

49. Zhang JX, Han L, Bao ZS et al (2013) HOTAIR, a cell cycle-associated long noncoding RNA and a strong predictor of survival, is preferentially expressed in classical and mesenchymal glioma. Neuro Oncol 15:1595–1603

50. Shi Y, Wang Y, Luan W et al (2014) Long non-coding RNA H19 promotes glioma cell invasion by deriving miR-675. PLoS ONE 9:e86295

51. Charo IF, Ransohoff RM (2006) The many roles of chemokines and chemokine receptors in inflammation. N Engl J Med 354:610–621

52. Karin N, Razon H (2018) Chemokines beyond chemo-attraction: CXCL10 and its significant role in cancer and autoimmunity. Cytokine. https://doi.org/10.1016/j.cyto.2018.02.012

53. Mirzaei H, Salehi H, Oskuee RK et al (2018) The therapeutic potential of human adipose-derived mesenchymal stem cells producing CXCL10 in a mouse melanoma lung metastasis model. Cancer Lett 419:30–39

54. Taslimi Y, Zahedifard F, Habibzadeh S et al (2016) Antitumor effect of IP-10 by using two different approaches: live delivery system and gene therapy. J Breast Cancer 19:34–44

55. Bronger H, Singer J, Windmuller C et al (2016) CXCL9 and CXCL10 predict survival and are regulated by cyclooxygenase inhibition in advanced serous ovarian cancer. Br J Cancer 115:553–563

56. D'Arcangelo D, Facchiano F, Nassa G et al (2016) PDGFR-alpha inhibits melanoma growth via CXCL10/IP-10: a multi-omics approach. Oncotarget 7:77257–77275